International Journal of Biotechnology Research ISSN: 0974-6293
Vol.11 No.1 january-June 2018

Mathematical Modeling of Tumor-Induced Angiogenesis Using Porous Medium Diffusion

THOMAS HORGER[1*#], AENNE OELKER[1], CHRISTINA KUTTLER[1***] & JUDITH PÉREZ-VELÁZQUEZ[2]**

ABSTRACT:

Background: Tumor angiogenesis is the process of vessel arousal and growth, initiated by chemical substances secreted by adjacent tissue of a tumor. After the tumor has reached a certain size, oxygen and nutrient supply cannot be accomplished alone by diffusion and the tumor forms new vessels from the adjacent tissue, which sprout and invade the tumor. The transition to this vascular stage is crucial to tumor development as it allows the tumor to grow and disseminate in the whole body.

The present work proposes a partial differential equations model which uses porous medium diffusion as well as Monod growth terms to model angiogenesis. Our hybrid model consists of two parts: in the first part, a continuous partial differential equations model is developed which describes how the concentrations of the factors inducing angiogenesis evolve in time, with equations for the concentration of the endothelial cells (EC), fibronectin, the matrix degenerating enzyme (MDE), and the concentration of tumor angiogenic factors (TAF). In the second part we model the motion of single sprouts by a random walk approach as a reaction to the underlying chemical field determined in the first part.

Results: With our model we are able to reproduce important features of angiogenesis like the brush border effect and the start of the tip proliferation at a certain concentration of TAF without the artificial use of Heaviside functions. We can see that the networks generated by our random walk model resemble vessel networks generated by angiogenesis *in vivo* (as seen in angiographic scans).

Conclusions: From our numerical simulations new possibilities to interpret the process of angiogenesis arise. The composition of the tissue can be considered by the use of different porosity constants, the higher this constant, the more collateral movement the simulated vessels show. Furthermore, the tip proliferation may no longer be the only reason for the brush border effect and the sudden increase of the EC density at certain concentrations since also the density of the tissue, which is modeled by the inclusion of porous medium diffusion, has to be considered.

KEYWORDS: Angiogenesis, Hybrid mathematical model, Porous medium, Reinforced random walk, Capillary formation, tumor growth

1. BACKGROUND

1.1 Introduction

Angiogenesis is the process of vessel arousal and growth, initiated by chemical substances secreted by adjacent tissue. In this paper we develop a mathematical model based on a system of nonlinear partial differential equations to describe the motion of the forming sprouts as a reaction to the underlying chemical

[1] Department of Mathematics, Technical University Munich, Boltzmannstr, 3, 85748 Garching, Germany, (*E-mails*: **thomas.horger@mytum.de*; ***aenne.oelker@mytum.de*; ****kuttler@ma.tum.de*)

[2] Institute of Computational Biology, Helmholtz Zentrum München, Ingolstädter Landstraße 1, 85764 Neuherberg, Germany, (*E-mail: perez-velazquez@helmholtz-muenchen.de*)

[#] Corresponding author

field induced by these chemical substances. The movement of the vessel tips towards the tumor is modeled by a biased random walk in which we assume the movement of the endothelial cells to depend on transition probabilities derived from the partial differential equations. Angiogenesis is a complex process with many factors involved; our model will focus on some of the key factors. Nevertheless, we are able to see that the numerical simulations generate vessels that resemble vessel networks produced by angiogenesis observable in angiographic scans. Moreover the important brush border effect, which reflects the fact that the main vessel density is behind the leading tip front and which is induced by the strong vessel branching in the proximity of the tumor, can be observed.

This work will be divided into two parts; in the first part we will develop a continuous mathematical model consisting of a set of partial differential equations which describes how the concentrations of the factors inducing the process of angiogenesis evolve in time. We choose to include the concentrations of the endothelial cells (EC), of fibronectin and of the matrix degenerating enzyme (MDE) as well as the concentration of tumor angiogenic factors (TAF) into our model. In the second part, we will model tumor angiogenesis by a random walk approach which describes the motion of the sprouts as a reaction to the underlying chemical field determined in the first part. It is based on the modeling framework called reinforced random walks [1], which was adapted to describe angiogenesis by Sleeman [2]. As a last step we will compare our results to vessel networks generated by angiogenesis *in vivo*.

In the first part of this paper, we will introduce the model in one dimension and then expand the model to two and three dimensions. In the second part of the paper, we will develop a random walk approach in two and three dimensions. The main focus in doing this is to develop a consistent model which will enable us to observe the effects of the inclusion of new terms in one as well as in two and three dimensional model settings. We will for example see how the assumption of Monod growth for the EC and the TAF and the use of porous media diffusion instead of conventional diffusion will improve the description of angiogenesis development.

1.2 Biological Background

Tumor development and growth evolve initially in two phases, an avascular and a vascular stage [3]. In the avascular stage, the tumor growth is restricted to few millimeters and its oxygen and nutrients supply takes place throughout diffusion. After the tumor has reached a certain size, oxygen and nutrient supply cannot be accomplished alone by diffusion and the tumor forms new vessels from the adjacent tissue, which sprout and invade the tumor. This stage is called vascular and it allows the tumor to grow and disseminate in the whole body. It was Folkman who first suggested [4] that the growth of a tumor beyond a certain size depends on its ability to recruit new blood vessels. Actual proof by direct observation of the process came until the late 1970's [5, 6].

The rise and growth of blood vessels is called angiogenesis and is essential for growth and reparative processes in tissues and organs. Blood vessels appear with the purpose of supplying tissues and organs with oxygen and nutrients [7]. In adults, most blood vessels remain dormant and angiogenesis becomes active in only a few physiologic situations (e.g. in the placenta during pregnancy for supplying the embryo with nutrients and in wound healing [7]). Tumor growth also requires angiogenesis. Vessel arousal and growth are initialized by chemical substances secreted by the tumor in the adjacent tissue. We will use the generic term tumor angiogenesis factor (TAF) to refer to these growth factors. Once this chemical process has been initiated, the extracellular matrix and the basal membrane begin to dissolve. After the basal membrane has been dissolved, the endothelial cells (EC) migrate out of the milieu towards the tumor. Simultaneously, the EC proliferate and form vessel-like structures. These vessel-like structures (sprouts) migrate towards the tumor. In this process, cell division is largely connected to an area just behind the sprout tip and interactions between the extracellular matrix and the cells strongly affect cell migration. One of the several matrix molecules

which are known to interact with the endothelial cells is fibronectin. It is especially important as it is known to enhance cell adhesion to the matrix. When fibronectin (and also TAF) bind to membrane receptors on the endothelial cells, cell migration is activated and as a consequence of this, the EC begin to produce a matrix degenerating enzyme (MDE) which increases the rate of attachment between EC and fibronectin.

In the next section, we give a brief overview of some mathematical models describing angiogenesis before we proceed to our model.

1.3 Mathematical Models of Angiogenesis

Angiogenesis is an important process in cancer growth as it is crucial to the attachment of the tumor to the blood system and thus also to the formation of metastases in the body. Therefore there has been great interest in modeling the process of angiogenesis and especially the role played by the EC and by the TAF has been studied extensively. Tumor-induced angiogenesis is a process which involves several scales, mathematical models describing all these different levels have been proposed. Our model is a hybrid model in which the progression of the vascular network is coupled to factors inducing the process of angiogenesis. This is a natural approach to achieve a description of angiogenesis as it deals with the relevant processes using an appropriate mathematical description for each.

Typically, mathematical models of angiogenesis describe the generation of a network of uncirculated proto-vessels. Among the best-known models are the works of Sleeman with Levin and later Planck [2, 8-16]. They used the idea of reinforced random walks and Michaelis Menten kinetics and have made a great contribution to modeling tumor induced angiogenesis. Their approach is based on Othmer and Stevens [17] and Davis [1]. They introduced their approach in [9]. This model described endothelial cell receptors as the stimulants for transforming angiogenic factor into proteolytic enzyme. A system of ordinary and partial differential equations (PDE) is derived to describe the aggregation of the EC and the collapse of the vascular lamina, which opens a passage into the extracellular matrix. This model was later extended in [11] to include the roles of pericytes and macrophages in regulating angiogenesis and included the presence of anti-angiogenic (angiostatic) factors. In [8] endothelial cell migration and proliferation into the extra-cellular matrix leading to angiogenesis were modeled. This model is a system of coupled nonlinear ordinary and PDEs. In [10] they focused on the biochemistry of the process at the level of the cell and propose standard transport equations for the diffusion of molecular species in porous media. A good agreement with observations from rabbit cornea experiments (onset of vascularization and the rate of capillary tip growth) was obtained.

In [2] reinforced random walks were used to model the chemotactic response of the EC to TAF. They also model the haptotactic response to the matrix macromolecule fibronectin using transition probability rate functions. These functions essentially assign directional probabilities for the movement of EC. Our model lies within this category.

Later, in [13], an individual cell-based model of tumor angiogenesis in response to a diffusible angiogenic factor is proposed. In [14] a cell-based mathematical model of an experiment is built to assess the response of EC to various diffusible angiogenic factors. The model includes both chemotaxis and chemokinesis. Two and three-dimensional simulations are carried out and the results correlate well with the experimental data. In [16] and [15] a mathematical description of the role of the angioproteins in angiogenesis is given. One of the most interesting points about these works is the access to experimental observations and the fact that the predictions of the model are in qualitative agreement. In [12] a circular random walk model is used to allow the cells to move independently of a lattice.

While in many cases, angiogenesis is considered in two-dimensional models, see for example Mantzaris, Webb and Othmer [18] and McDougall, Anderson and Chaplain [19], there exist three-dimensional models,

like Chaplain [20]. Many three-dimensional models focus on considering the evolution of TAF and EC in time, while the model of Chaplain also includes fibronectin. In McDougall, Anderson, Chaplain, in addition to that, the effect of the matrix degenerating enzyme is taken into account. The model developed by Anderson, Chaplain, GarcReimbert and Vargas [21] as well as the model by Mantzaris, Webb and Othmer [18] also investigate the role played by angiostatin.

While today most models are hybrid, early models may be divided into discrete and continuous models, including a continuous part dedicated to the description of a system of (partial) differential equations modeling the evolution of the underlying chemicals as well as a discrete part in which a random walk model is used to simulate the evolution of particular vessels in space and time. Examples for the continuum models are Balding and McElwain [22], H. M. Byrne and M. A. J. Chaplain [23], M. A. J. Chaplain [24], J. Valenciano [25] and M. E. Orme and M. A. J. Chaplain [26]. These models consist of partial differential equations, and describe macroscopic quantities like sprout density, tip density and network expansion rates. Among the discrete type are Stéphanou *et al*., [27] and the already mentioned works of Sleeman and others. These models contained stochastic elements and have the advantage of following the motion of an individual endothelial cell. They are also able to generate a realistic capillary network structure. An example of a hybrid model is the one proposed by Anderson and Chaplain [28]. More recent models include multi-scale phase-field models [29], multi-compartment models [30], among others. For relatively recent reviews of the progress in the field of angiogenesis modeling see for example [31] and [32].

In our model, we include the effects of the changes of EC, TAF, fibronectin and MDE concentrations in time on the development of sprouts towards the tumor. We will work in a three dimensional setting and, in contrast to most of the models mentioned above, assume that the diffusion we observe may be modeled as a porous medium diffusion. McDougall and Sorbie [33] have used porous medium diffusion in the context of petroleum engineering, modeling the flow of water, gas and oil through porous rock. The use of the porous medium diffusion in the context of angiogenesis accounts for the consistence of tissue in the human body, which, like porous rock, does not allow for material to move freely but restricts it to a microvascular network in which diffusion can take place. The composition of human tissue, which is much different from that of porous rock, is taken into account by the use of a porosity constant in the porous medium equation.

Porous medium equations have been used in the context of angiogenesis, though in a different approach, for example in [34] for an equation for the extracellular matrix (ECM) which is regarded as porous material. Similarly, Zheng *et al*., [35] modeled the tumor cells at the continuum level as a viscous fluid flowing through a porous medium (extracellular matrix). Sleeman and Levine [36] also considered the ECM as a porous medium. In [10] was also assumed that the ECM is a porous medium through which chemicals can diffuse. Although not in the context of angiogenesis, following the modeling framework of [37], Byrne and Preziosi [38] developed a mathematical model describing an avascular tumor as a saturated porous material. Habbal [39] considered the vessel-matrix-tumor system as a porous medium from the tumor viewpoint and as an elastic structural medium from the host tissue viewpoint, with both the ECM and the tumoral vasculature as a porous medium.

2. Continuous Mathematical Model

Our continuous mathematical model consists of a system of four partial differential equations describing the evolution of the concentrations of the endothelial cells, the tumor angiogenic factors, fibronectin and the matrix degenerating enzyme in time.

2.1 Derivation of the PDE-System

Following [28], we assume the motion of the endothelial cells to be influenced by random motility, chemotaxis and haptotaxis. Thus, the flux will be assumed to be

$$J = J_{\text{random}} + J_{\text{chemo}} + J_{\text{hapto}}$$

$$= -D_n \left(\frac{n}{n_0} \right)^{\sigma} \nabla n + n\chi_0 \nabla c + \varphi n \nabla f \, .$$

We model the diffusion of the EC as a porous medium diffusion, which accounts for the composition of human tissue and is a novel component of our model. A porous medium is a material containing pores (voids), which are typically filled with a fluid, and a matrix, which is usually a solid. Here, we use the porous medium diffusion because it allows us to model the inherent resistance of the tissue to the diffusing substances and endothelial cells. In order to diffuse in the tissue of the human body, a certain amount of the substances or EC must be available such that the "pressure" needed to penetrate the tissue can be built up. A porous medium is most often characterised by its porosity. We choose D_n to be the diffusion coefficient of the endothelial cell concentration n and σ to be the porosity constant mentioned before. The Fickian diffusion is included into our model as a special case; it is obtained if $\sigma = 0$. The chemotactic flux component reflects the influence of changes in the TAF concentration c on the EC concentration. As a simplification, we suppose the chemotactic function $\chi(c)$ to be constant. In the differential equation, we also account for the influence of haptotaxis, where φ is the rate of haptotactic cell migration and f is the fibronection concentration, and the cell loss with death rate κ. Furthermore, we will assume that the changes of EC and TAF concentrations are linked by a process called Monod growth. This means that the growth rate of the endothelial cells is restricted by the concentration of a "limiting nutrient", which is in this case the TAF. A Monod growth process is of the following form:

$$\frac{dx}{dt} = x\mu_m \frac{s}{K_s + s},$$

where x is the concentration of the substance we consider, s is the concentration of the limiting nutrient, μ_m is the maximum specific growth rate and K_s is the substrate concentration that supports half-maximum specific growth rate.

We get the following equation for the change of the endothelial cell concentration in time, which we will need in the second part of our model in order to deduce a random walk model of angiogenesis:

$$\frac{\partial n}{\partial t} = D_n \nabla \left(\left(\frac{n}{n_0} \right)^{\sigma} \nabla n \right) - \nabla (\chi_0 n \nabla c) - \varphi \nabla (n \nabla f) - \kappa n + \mu_2 n \frac{c}{\gamma_2 + c} \, .$$

As we have seen above, the change of the endothelial cell concentration depends on several factors which will themselves need to be described by partial differential equations. When considering the change of the TAF concentration in time, we include a diffusion term with diffusion coefficient D_c into our model. In higher dimensions, the diffusion coefficient becomes a diagonal matrix with positive constant diffusion coefficients. In addition to that, the decay of TAF with associated decay coefficient δ and a Monod growth term, which reflects the fact that the concentration of TAF decreases if the EC density is high, are included.

These processes are modeled by the following equation:

$$\frac{\partial c}{\partial t} = D_c \nabla^2 c \; - \delta c - \frac{\alpha_1 c n}{\gamma_1 + c} \, .$$

Next, we investigate the change of the fibronectin concentration f in time. In doing so, we take into account the production of fibronectin by the EC with production constant β as well as the uptake and

binding of fibronectin to the EC as they migrate towards the tumor with uptake constant μ. Additionally, the effect of the concentration of MDE (matrix degenerating enzyme) m, which enhances the attachment of the cells to fibronectin, with coefficient η is considered. We do not consider diffusion of the fibronectin as it is produced and also consumed only by the vessels. This results in the following equation for the fibronectin concentration:

$$\frac{\partial f}{\partial t} = \beta n - \mu n f - \eta m f .$$

The change of the MDE density in time is modeled according to McDougall, Anderson and Chaplain [19]. In this model, the change of MDE depends on the production of MDE by the EC with production rate α as well as the diffusion of MDE with diffusion coefficient τ and the spontaneous degradation of MDE at rate ν. This is modeled as follows:

$$\frac{\partial m}{\partial t} = \alpha n + \tau \nabla^2 m - \nu m .$$

Taking into account all factors, we obtain the following set of four partial differential equations:

$$\begin{aligned}
\frac{\partial n}{\partial t} &= D_n \nabla \left(\left(\frac{n}{n_0} \right)^{\sigma} \nabla n \right) - \nabla (\chi_0 n \nabla c) - \varphi \nabla (n \nabla f) - \kappa n + \mu_2 n \frac{c}{\gamma_2 + c} \\
\frac{\partial c}{\partial t} &= D_c \nabla^2 c - \delta c - \frac{\alpha_1 c n}{\gamma_1 + c} \\
\frac{\partial f}{\partial t} &= \beta n - \mu n f - \eta m f \\
\frac{\partial m}{\partial t} &= \alpha n + \tau \nabla^2 m - \nu m .
\end{aligned} \tag{1}$$

For our calculations in one dimension, we easily deduce the following one-dimensional system of partial differential equations:

$$\begin{aligned}
\frac{\partial n}{\partial t} &= D_n \frac{\partial}{\partial x} \left(\left(\frac{n}{n_0} \right)^{\sigma} \frac{\partial n}{\partial x} \right) - \frac{\partial}{\partial x} \left(\chi_0 n \frac{\partial c}{\partial x} \right) - \frac{\partial}{\partial x} \left(\varphi n \frac{\partial f}{\partial x} \right) - \kappa n + \mu_2 n \frac{c}{\gamma_2 + c} \\
\frac{\partial c}{\partial t} &= D_c \frac{\partial^2 c}{\partial x^2} - \delta c - \frac{\alpha_1 c n}{\gamma_1 + c} \\
\frac{\partial f}{\partial t} &= \beta n - \mu n f - \eta m f \\
\frac{\partial m}{\partial t} &= \alpha n + \tau \frac{\partial^2 m}{\partial x^2} - \nu m .
\end{aligned} \tag{2}$$

2.2 Initial and Boundary Conditions

In order to perform numerical simulations, we want to choose appropriate initial and boundary conditions. We will first comment on the deduction of the initial and boundary conditions in one dimension and then explain, how the two- and three-dimensional settings are derived.

In our setting, the tumor is located at position $x = 0$ and the vessel is at $x = 1$. Before the basal membrane is dissolved and the endothelial cells (EC) begin to migrate out of the milieu towards the tumor, there are no endothelial cells in the system except for the vessel area. This is reflected by condition (3a). Fibronectin is a native ECM protein and thus assumed to be initially present everywhere at a small initial concentration ε_0 and higher at the vessel (3c). Initially, the concentration of the MDE is assumed to be zero (3d) which reflects the fact that MDE is generated by the endothelial cells. Furthermore, the tumor secretes TAF in order to initiate angiogenesis. Thus, we assume that the initial concentration of TAF is dependent on the distance to the tumor, which may be seen in condition (3b). This condition was chosen according to [24]. We use the following initial conditions on the concentrations of the substances under consideration:

$$n(0, x) = \begin{cases} n_0, & x = 1, \\ 0, & x < 1. \end{cases} \tag{3a}$$

$$c(0, x) = c_0(x) = 1 - x^2 \tag{3b}$$

$$f(0, x) = \begin{cases} f_0, & x = 1, \\ \varepsilon_0, & x < 1. \end{cases} \tag{3c}$$

$$m(0, x) = 0. \tag{3d}$$

During angiogenesis, several boundary conditions assure that the natural setting is reflected properly. We have to assume that the vessel will emit endothelial cells for the whole duration of the process of angiogenesis in order to ensure the ongoing of the vessel growth and that the endothelial cells will always emit fibronectin. Furthermore, we will assume that the tumor will always emit TAF and that the TAF will be consumed on its way to the vessel. On the other boundaries, we impose a no-flux boundary condition, choosing an outward unit normal vector ξ. This may be interpreted in two different ways: it may reflect the assumption that the EC, and thus also the sprouts, will remain in the domain under consideration or the assumption that the same conditions apply to the area outside the domain under consideration such that there is no flow on the boundaries. All of this will be reflected in the following boundary conditions:

$$n(t, 1) = n_0, \quad c(t, 0) = c_b, \quad c(t, 1) = 0, \quad f(t, 1) = f_0.$$

When we expand our setting to two and three dimensions, we assume that the tumor is located in the middle of the left side of the domain and that the vessel is located at the right side of the domain. Most of the initial and boundary conditions are very similar and we adapted the initial concentration of TAF to be $c(0, x, y) = c_0(x, y) = \frac{1.25 - (x^2 + (y - 0.5)^2)}{1.25}$ and $c(0, x, y, z) = c_0(x, y, z) = \frac{1.5 - (x^2 + (y - 0.5)^2 + (z - 0.5)^2)}{1.5}$ in two and three dimensions respectively.

2.3 Numerical Results

2.3.1 *One Dimension*

For our one-dimensional numerical simulations we choose the domain to be [0, 1], divided into 100 grid points, and consider 20000 time steps. We discretise our equations using finite difference approximations and take into account the boundary and initial conditions mentioned above. Since our simulations are intended to show qualitative rather than quantitative results, we chose the parameters similar to the ones used in [24], the missing ones were chosen in similar order to allow for a qualitative analysis. The non-dimensional parameters used in simulations were $D_c = 1$, $\alpha_1 = 10$, $\gamma_1 = 1$, $\delta = 1$, $D_n = 0.1$, $\sigma = 4$, $n_0 = 1$, $\chi_0 = 1$, $\kappa = 5$, $\mu_2 = 20$, $\gamma_2 = 0.7$, $\varphi = 0.004$, $f_0 = 1$, $\beta = 5$, $\mu = 0.1$, $\eta = 1$, $\alpha = 1$, $\tau = 1$ and $\nu = 1$. Such a choice of parameters results in the concentration profiles for endothelial cells, TAF, fibronectin and MDE of Fig. 1. When considering the development of the EC concentration in Fig. 1(a) at a time when EC get to the tumor,

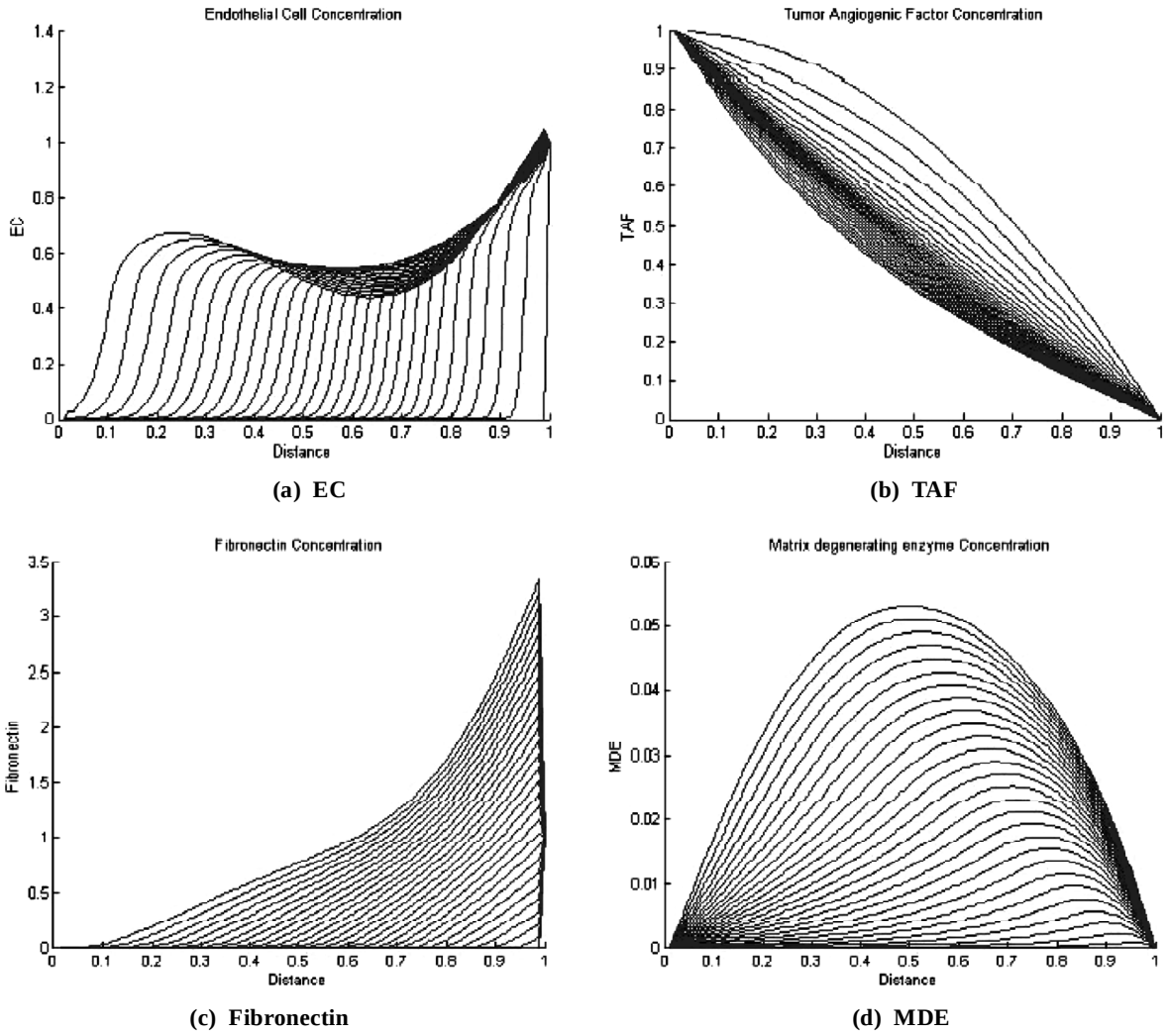

(a) EC **(b) TAF**

(c) Fibronectin **(d) MDE**

Figure 1: Simulation Results for Equations (2) ($\sigma = 4$)

we can observe that the concentration of EC near the vessel is fairly high, then it decreases and rises again, as we get closer to the tumor. The diffusion of the endothelial cells towards the tumor is inhibited by the tissue until a certain pressure is built. This is a natural result of the porous medium diffusion and the Monod growth in our model and does not have to be pre-imposed by the use of a Heaviside function. Furthermore, we can observe the start of a strong tip proliferation in Fig. 1(a) around distance 0.6: Until a certain concentration of TAF is reached, the EC do not split so often, but when this concentration is reached, the sprouts begin to proliferate and the concentration of endothelial cells rises dramatically. We also reproduce the very important brush border effect which means that the there is a high EC density behind the leading tip front.

When choosing different values for σ in Fig. 2, the effect of the inclusion of the porous media diffusion into our model becomes more obvious; if we choose $\sigma = 0$ we obtain the result we would have obtained when working with conventional diffusion. In this sense our model is more general. The endothelial cells can diffuse without being stopped by the tissue. When we increase the porosity constant to higher values, we can observe that it becomes more and more dicult for the EC to reach the tumor. For a value of $\sigma = 10$, one can observe how the EC have no chance of reaching the tumor unless they have accumulated enough pressure to force their way through the porous tissue. When increasing the porosity constant even further, one can see that the EC are even held back on their way to the tumor and with a constant of $\sigma = 19$, we see how the migration of the EC stops at a very early stage of the process, which may be seen in Fig. 2(d). In Fig. 2(a) and (b), one can see that the brush border effect becomes more obvious with increasing σ. We also

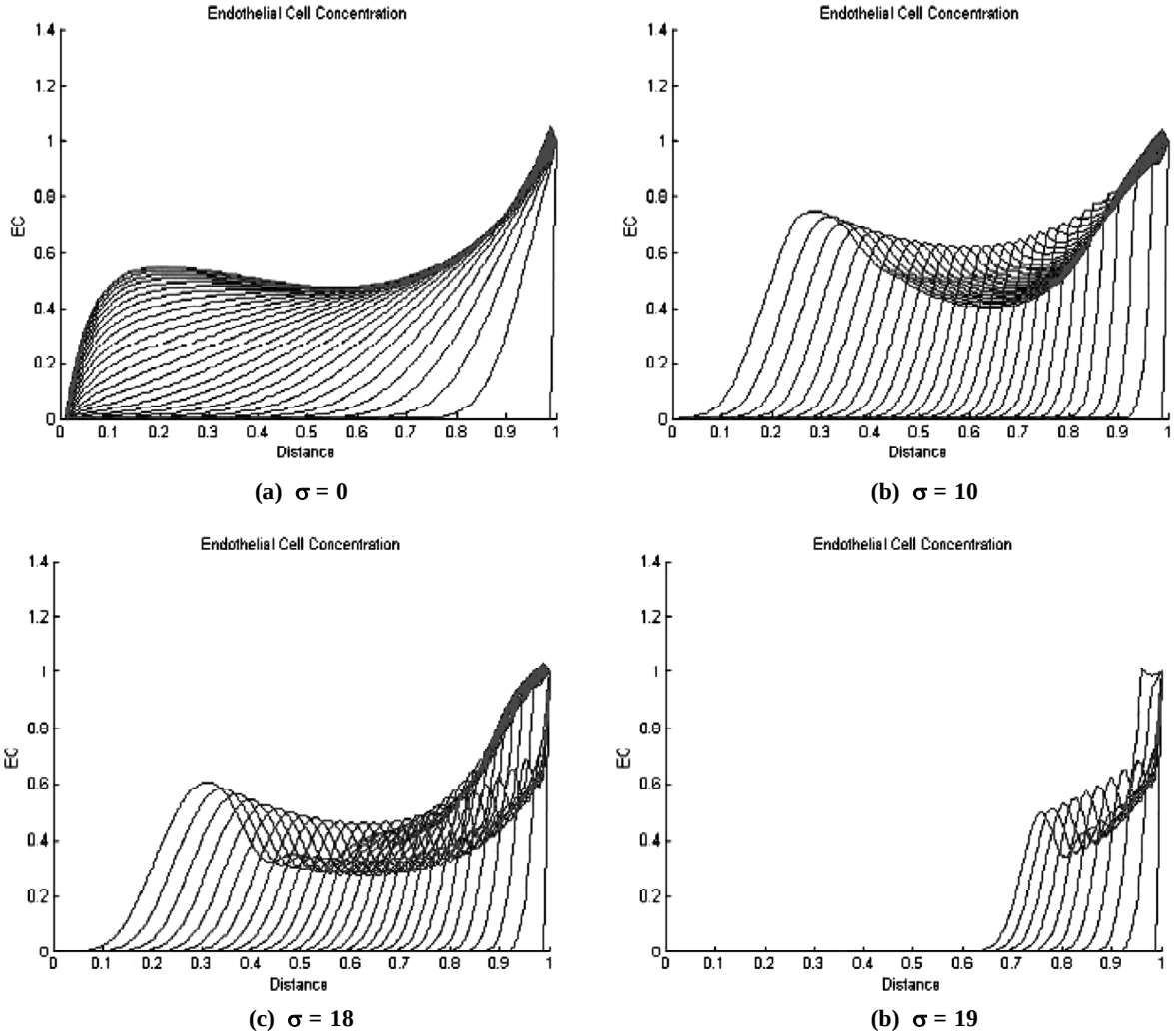

(a) $\sigma = 0$ **(b) $\sigma = 10$**

(c) $\sigma = 18$ **(b) $\sigma = 19$**

Figure 2: Simulation Results for Equations (2) for Different Values of σ in One Dimension

observe in Fig. 1(b) that the more EC, the more TAF is consumed until the concentration of the TAF reaches a kind of steady state, which means a state whose changes are so small that they can be neglected. This is why, as a simplification, one could also assume an *a priori* concentration when developing a model of tumor angiogensis. The concentration of fibronectin is very high in proximity of the original vessel and then decreases rapidly towards the tumor as the fibronectin is needed in the process of sprout formation, which is seen in Fig. 1(c). In addition to that, Fig. 1(d) shows that the concentration of MDE is high around the sprouts as it is produced by the EC. Once produced, the MDE diffuses into the surrounding tissue but is not consumed as it is an enzyme.

2.3.2 *Two Dimensions*

When working in the two-dimensional setting, we choose our domain to be $[0, 1] \times [0, 1]$, each side divided into 50 steps. Also we work with 60000 time steps. In Figs. 3 and 4, we will illustrate how the substance concentrations in two dimensions have evolved after 40000 timesteps, which is two thirds of the timesteps we are considering. For better comparability we have chosen the parameters in the same way as we did in one dimension, especially we chose $\sigma = 4$. One can see that the qualitative course of development of the concentrations is the same as in one dimension, compare Figs. 1 and 3. We can see the brush border effect, the tip proliferation, the concentration of TAF, the fibronectin decay as well as the fact that most of the MDE can be found in the area of the sprouts, which is in agreement with reality as the MDE is produced by

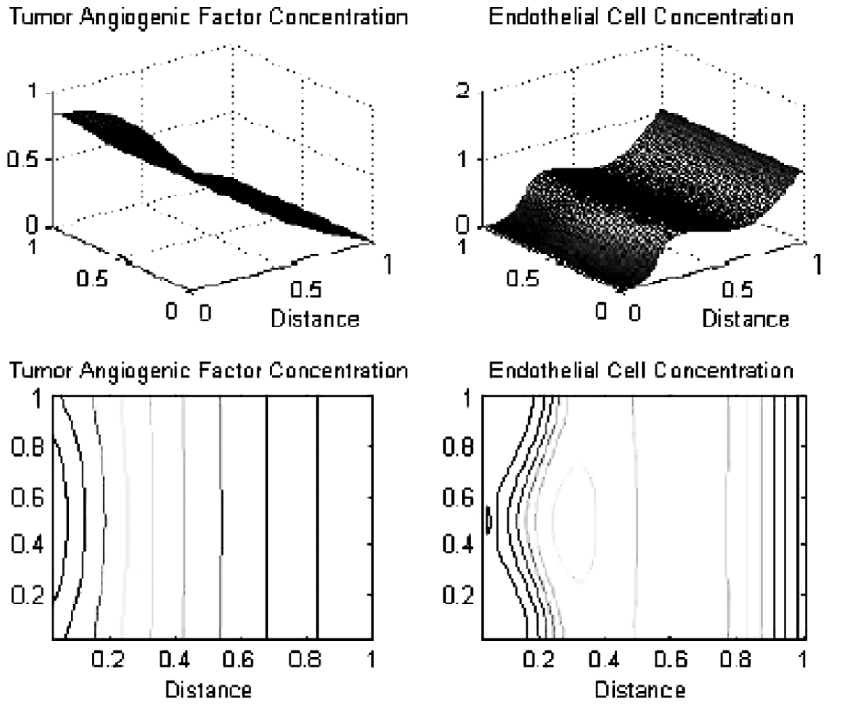

(a) TAF and EC

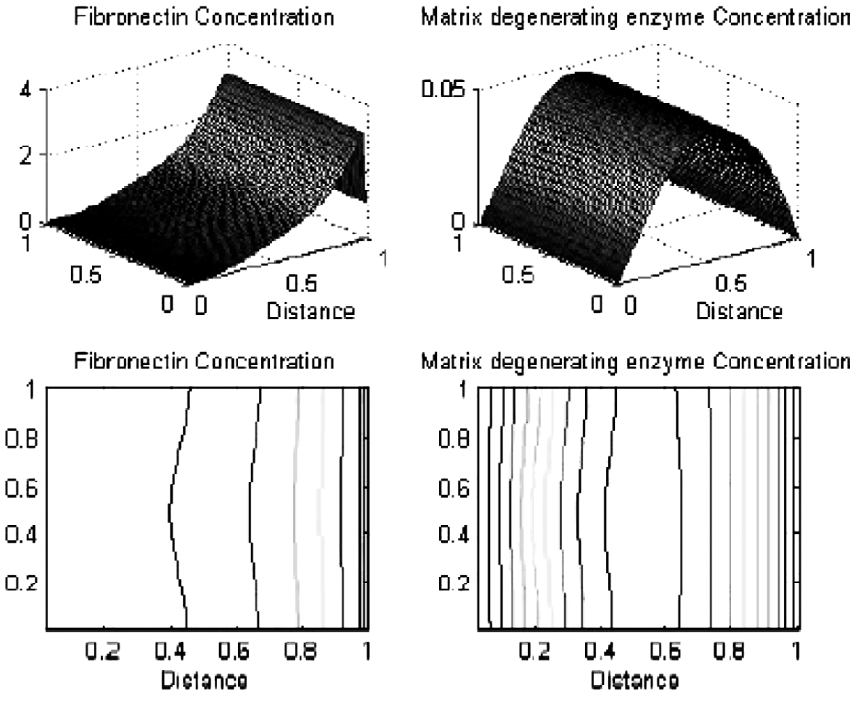

(b) fibronectin and MDE

Figure 3: Graphs and Contour Plots for $\sigma = 4$ in Two Dimensions

the EC. Furthermore, the same differences between the assumptions of classic and porous medium diffusion become obvious, compare Figs. 3 and 4. In addition to that, the attraction of the endothelial cells by the tumor can easily be observed in the surface plot of the endothelial cell concentration in Fig. 3. When comparing this surface plot to the surface plot of the endothelial cells in Fig. 4, i.e., the surface plot of the EC for $\sigma = 0$, we observe that the attraction of the EC by the tumor is weaker, which is due to the porous medium diffusion.

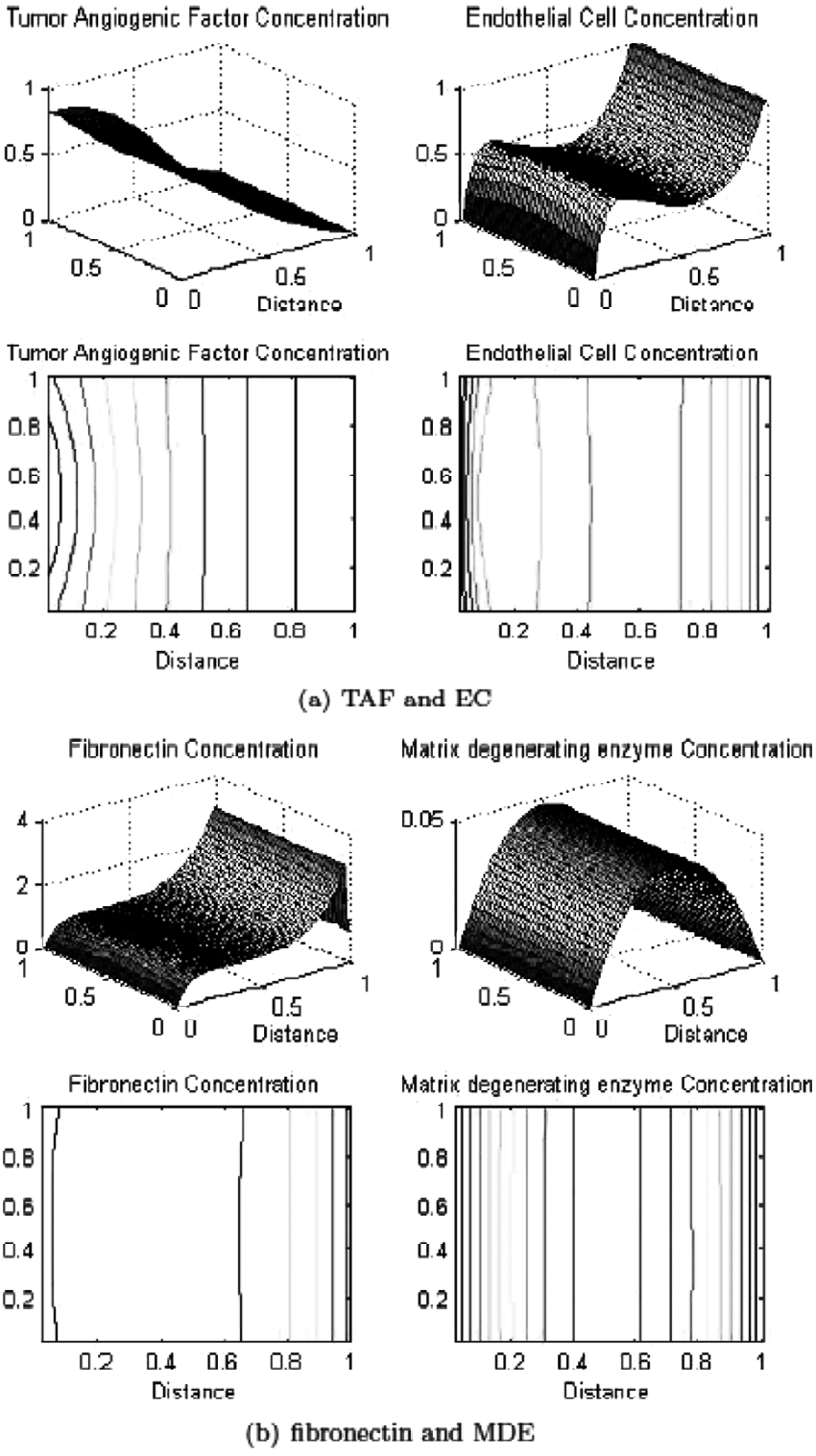

Figure 4: Graphs and Contour Plots for $\sigma = 0$ in Two Dimensions

2.3.3 *Three Dimensions*

In three dimensions, we want our domain to be $[0, 1]^3$, each side divided into 20 steps. We consider 20000 timesteps. Again, we leave the parameters like they were in one and two dimensions. As we now have to consider a three-dimensional domain, we draw a scatterplot assigning colors to different concentration levels on the grid points. The resulting images of the distributions of the concentrations may be seen in Fig. 5.

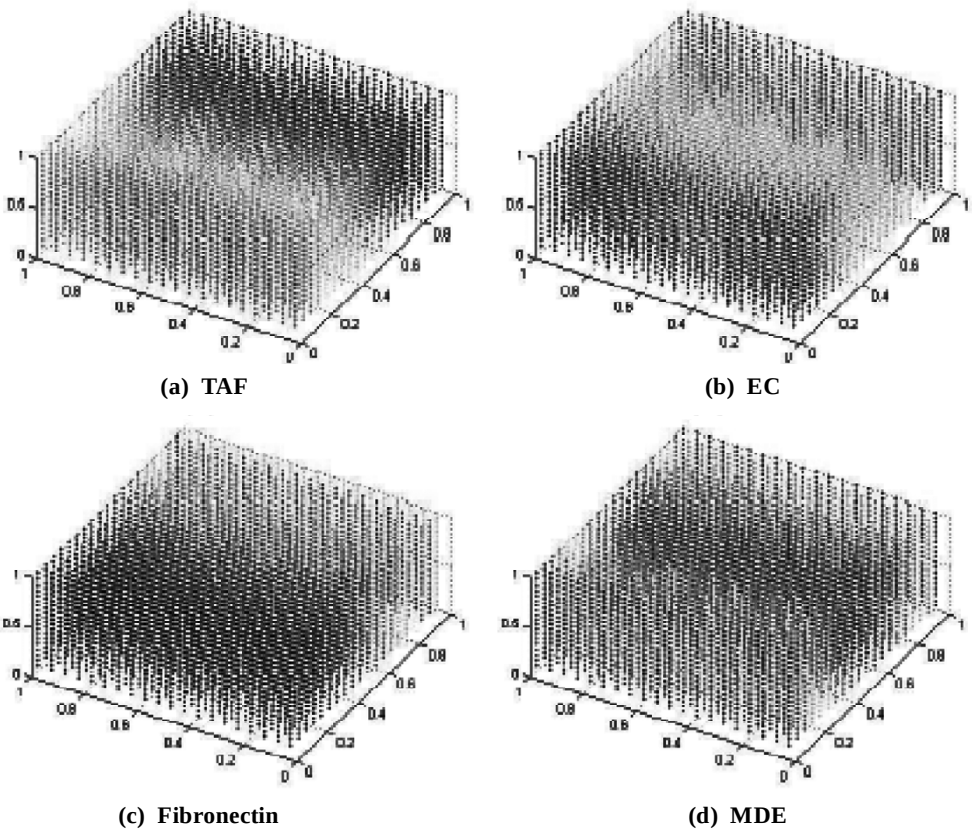

(a) TAF (b) EC

(c) Fibronectin (d) MDE

Figure 5: Three-Dimensional Scatterplots for σ = 4

We again see the decay of the concentrations and the high concentration of MDE around the sprouts. The three-dimensional images in Fig. 5 are difficult to interpret due to the fact that one cannot see all points at once, but we can consider cross-sections of the three-dimensional images. When considering these cuts, we also see that our three-dimensional model is in agreement with the two-dimensional version as the cut we consider looks just like the simulation results from the two-dimensional model. This is visualized in Fig. 6 which shows a cut through the middle of the three-dimensional plot of the endothelial cell concentration at timestep 9000 of 20000.

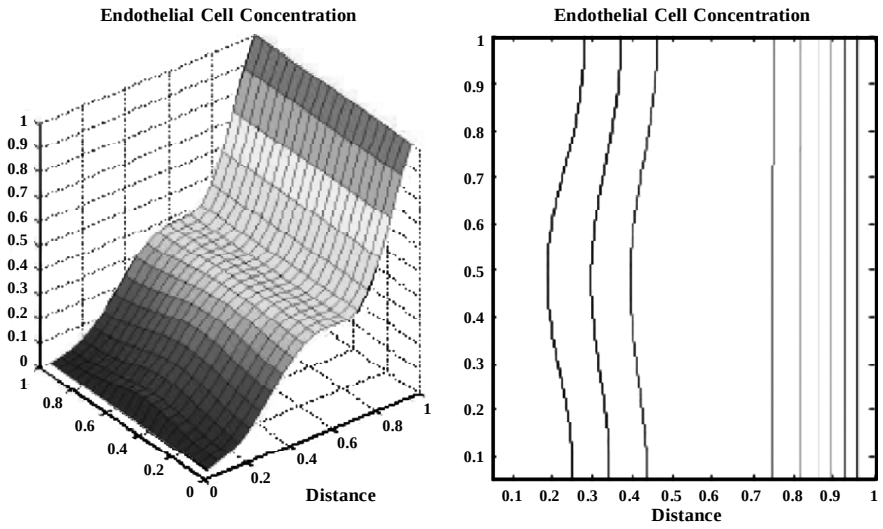

Figure 6: Two-Dimensional Cut Through the Middle of the Three-Dimensional Scatterplot of the EC for σ = 4 at Timestep 9000 of 20000

3. DISCRETE MATHEMATICAL MODEL

The second part of our model consists in applying a random walk setting, where the probabilities of moving in one special direction depend on the underlying concentration profiles of the substances investigated in the first section. In this setting we will assume that the probabilities of moving forward or backward, left or right and up or down are independent of each other where each single decision is triggered by the underlying concentration. By comparison of coefficients, we will get expressions which are proportional to the probabilities we are looking for.

3.1 Random Walk Model

In this section we will try to model the paths of individual endothelial cells using the discretisation of our system of partial differential equations (1). By comparison of coefficients we obtain probabilities of movement for an individual cell from the coefficients of the five-point finite-difference stencil in two or the seven-point finite-difference stencil in three dimensions. In order to be able to apply the method of comparison of coefficients, we chose $\sigma = 0$ in our partial differential equations, i.e., ordinary diffusion. However, this will not signicantly change the outcome of our random walk model as we will still apply the concentrations from the equations with porous medium diffusion. The concentration of EC at one special grid point at timestep $t + 1$ is the sum of the concentrations of EC at time t at all grid points which allows a transition to this grid point times the probabilities of moving to this grid point. Thus, the two-dimensional case is illustrated by the following equation:

$$n_{i,j}^{t+1} = n_{i,j}^{t} P_0 + n_{i+1,j}^{t} P_1 + n_{i-1,j}^{t} P_2 + n_{i,j+1}^{t} P_3 + n_{i,j-1}^{t} P_4.$$

For the coefficient P_0 of no movement we obtain the following form

$$\begin{aligned} P_0 = 1 &- \frac{4\varepsilon D_n}{h^2} - \frac{\varepsilon\chi_0}{h^2}\left(c_{i+1,j}^{t} + c_{i-1,j}^{t} - 4c_{i,j}^{t} + c_{i,j+1}^{t} + c_{i,j-1}^{t}\right) \\ &- \frac{\varepsilon\varphi}{h^2}\left(f_{i+1,j}^{t} + f_{i-1,j}^{t} - 4f_{i,j}^{t} + f_{i,j+1}^{t} + f_{i,j-1}^{t}\right) - \kappa + \frac{\mu_2 c_{i,j}^{t}}{\gamma_2 + c_{i,j}^{t}}, \end{aligned}$$

while the coefficients P_1, P_2, P_3 and P_4 which are proportional to the probabilities of moving right, left, up and down, may be written as:

$$\begin{aligned} P_1 &= \frac{\varepsilon D_n}{h^2} - \frac{\chi_0\varepsilon}{4h^2}\left(c_{i+1,j}^{t} - c_{i-1,j}^{t}\right) - \frac{\varphi\varepsilon}{4h^2}\left(f_{i+1,j}^{t} - f_{i-1,j}^{t}\right), \\ P_2 &= \frac{\varepsilon D_n}{h^2} + \frac{\chi_0\varepsilon}{4h^2}\left(c_{i+1,j}^{t} - c_{i-1,j}^{t}\right) + \frac{\varphi\varepsilon}{4h^2}\left(f_{i+1,j}^{t} - f_{i-1,j}^{t}\right), \\ P_3 &= \frac{\varepsilon D_n}{h^2} - \frac{\chi_0\varepsilon}{4h^2}\left(c_{i,j+1}^{t} - c_{i,j-1}^{t}\right) - \frac{\varphi\varepsilon}{4h^2}\left(f_{i,j+1}^{t} - f_{i,j-1}^{t}\right), \\ P_4 &= \frac{\varepsilon D_n}{h^2} + \frac{\chi_0\varepsilon}{4h^2}\left(c_{i,j+1}^{t} - c_{i,j-1}^{t}\right) + \frac{\varphi\varepsilon}{4h^2}\left(f_{i,j+1}^{t} - f_{i,j-1}^{t}\right). \end{aligned}$$

Analogously to the two-dimensional case, we assume for the three-dimensional case

$$n_{i,j,k}^{t+1} = n_{i,j,k}^{t} P_0 + n_{i+1,j,k}^{t} P_1 + n_{i-1,j,k}^{t} P_2 + n_{i,j+1,k}^{t} P_3 + n_{i,j-1,k}^{t} P_4 + n_{i,j,k+1}^{t} P_5 + n_{i,j,k-1}^{t} P_6.$$

While the coefficient of no movement P_0 may be written as

$$P_0 = 1 - \frac{6\varepsilon D_n}{h^2} - \frac{\varepsilon\chi_0}{h^2}(c^t_{i+1,j,k} + c^t_{i-1,j,k} - 6c^t_{i,j,k} + c^t_{i,j+1,k} + c^t_{i,j-1,k} + c^t_{i,j,k+1} + c^t_{i,j,k-1})$$
$$- \frac{\varepsilon\varphi}{h^2}(f^t_{i+1,j,k} + f^t_{i-1,j,k} - 6f^t_{i,j,k} + f^t_{i,j+1,k} + f^t_{i,j-1,k} + f^t_{i,j,k+1} + f^t_{i,j,k-1}) - \kappa + \frac{\mu_2 c^t_{i,j,j}}{\gamma_2 + c^t_{i,j,k}},$$

we get for the coefficients P_1, P_2, P_3, P_4, P_5 and P_6 of moving right, left, up, down, back and forth

$$P_1 = \frac{\varepsilon D_n}{h^2} - \frac{\chi_0\varepsilon}{4h^2}(c^t_{i+1,j,k} - c^t_{i-1,j,k}) - \frac{\varphi\varepsilon}{4h^2}(f^t_{i+1,j,k} - f^t_{i-1,j,k}),$$

$$P_2 = \frac{\varepsilon D_n}{h^2} + \frac{\chi_0\varepsilon}{4h^2}(c^t_{i+1,j,k} - c^t_{i-1,j,k}) + \frac{\varphi\varepsilon}{4h^2}(f^t_{i+1,j,k} - f^t_{i-1,j,k}),$$

$$P_3 = \frac{\varepsilon D_n}{h^2} - \frac{\chi_0\varepsilon}{4h^2}(c^t_{i,j+1,k} - c^t_{i,j-1,k}) - \frac{\varphi\varepsilon}{4h^2}(f^t_{i,j+1,k} - f^t_{i,j-1,k}),$$

$$P_4 = \frac{\varepsilon D_n}{h^2} + \frac{\chi_0\varepsilon}{4h^2}(c^t_{i,j+1,k} - c^t_{i,j-1,k}) + \frac{\varphi\varepsilon}{4h^2}(f^t_{i,j+1,k} - f^t_{i,j-1,k}),$$

$$P_5 = \frac{\varepsilon D_n}{h^2} - \frac{\chi_0\varepsilon}{4h^2}(c^t_{i,j,k+1} - c^t_{i,j,k-1}) - \frac{\varphi\varepsilon}{4h^2}(f^t_{i,j,k+1} - f^t_{i,j,k-1}),$$

$$P_6 = \frac{\varepsilon D_n}{h^2} + \frac{\chi_0\varepsilon}{4h^2}(c^t_{i,j,k+1} - c^t_{i,j,k-1}) + \frac{\varphi\varepsilon}{4h^2}(f^t_{i,j,k+1} - f^t_{i,j,k-1}).$$

At this point it is necessary to consider the tip proliferation. Therefore, we will use different probabilities, depending on the distance from the tumor, for the forming of new sprouts out of already existing ones. We assume that new sprouts can only be formed by already existing sprouts. Furthermore, we assume that the newly formed sprouts are not instantly branching onwards. We further assume that a new sprout can form from an existing sprout with a certain probability. This probability depends on the TAF-concentration and the probability that it branches onwards is increasing with the TAF-concentration. Therefore, we select the probability in the following way: near the vessel there is no branching. The probability of branching in a certain distance, respectively concentration, is slowly increasing, until near to the tumor, a high probability of branching exists and the so-called brush border effect occurs.

3.2 Numerical Results

In this section we present the results of our simulation. At this stage we want to note that the description is qualitative and therefore the parameters chosen for the model aim to illustrate and describe the global behavior. Numerical simulations have been produced using Matlab (Mathworks). The random walk model described above produces the following images which may be viewed as examples of the process of angiogenesis if this process takes place as described by the model equations from the first section. We can choose the number of sprouts which are going to form from the blood vessel. In Fig. 7 we choose the number of sprouts to be one, two and three and we also show the resulting images for $\sigma = 0$ and $\sigma = 4$, i.e., the underlying concentrations are modeled using ordinary diffusion or porous medium diffusion. We observe that when using the same parameters except for σ, in the simulations with porous medium diffusion, i.e., $\sigma = 4$, there is more movement up and down than in the simulations with ordinary diffusion. Furthermore,

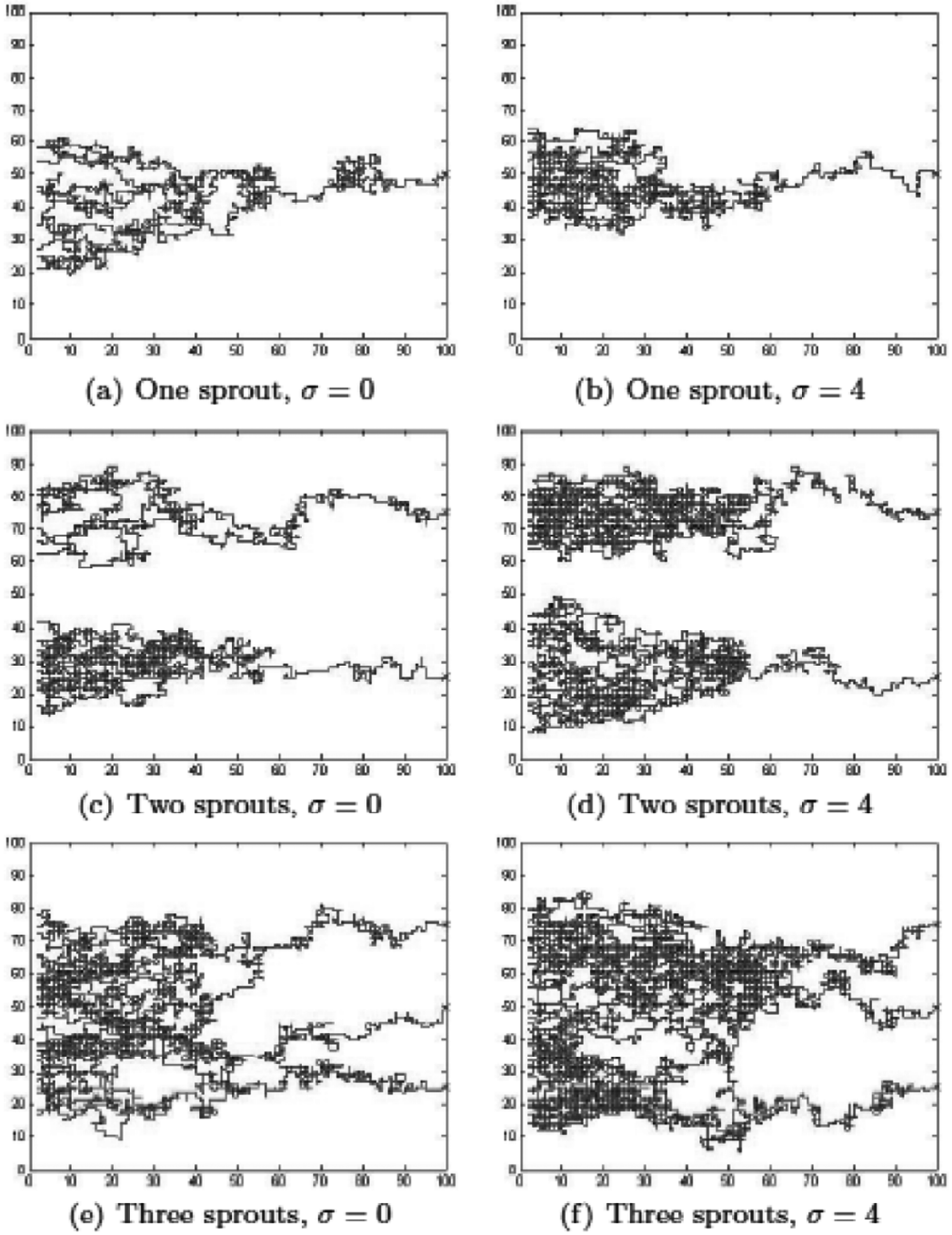

Figure 7: Two-Dimensional Random Walk Images for Different Number of Sprouts and Different Values of σ

we see that the sprouts are drawn towards the tumor more strongly. This is due to the fact that a certain pressure has to be built up before the substances can advance in the tissue when using porous medium diffusion.

In Figure 7, one can see how the sprouts are drawn towards the tumor which is in the middle of the left side domain. We expected such behaviour from the two-dimensional graphs and contour plots of the substances under consideration. Furthermore, it also becomes visible that the sprouts show a straighter growth movement the closer they get to the tumor and in addition to that, the brush border effect can be observed as the maximum tip density is located behind the leading front. Also, the tip proliferation and the fact that it becomes stronger the closer we get to the tumor can be seen. After a certain concentration of TAF is exceeded, tip proliferation starts to happen.

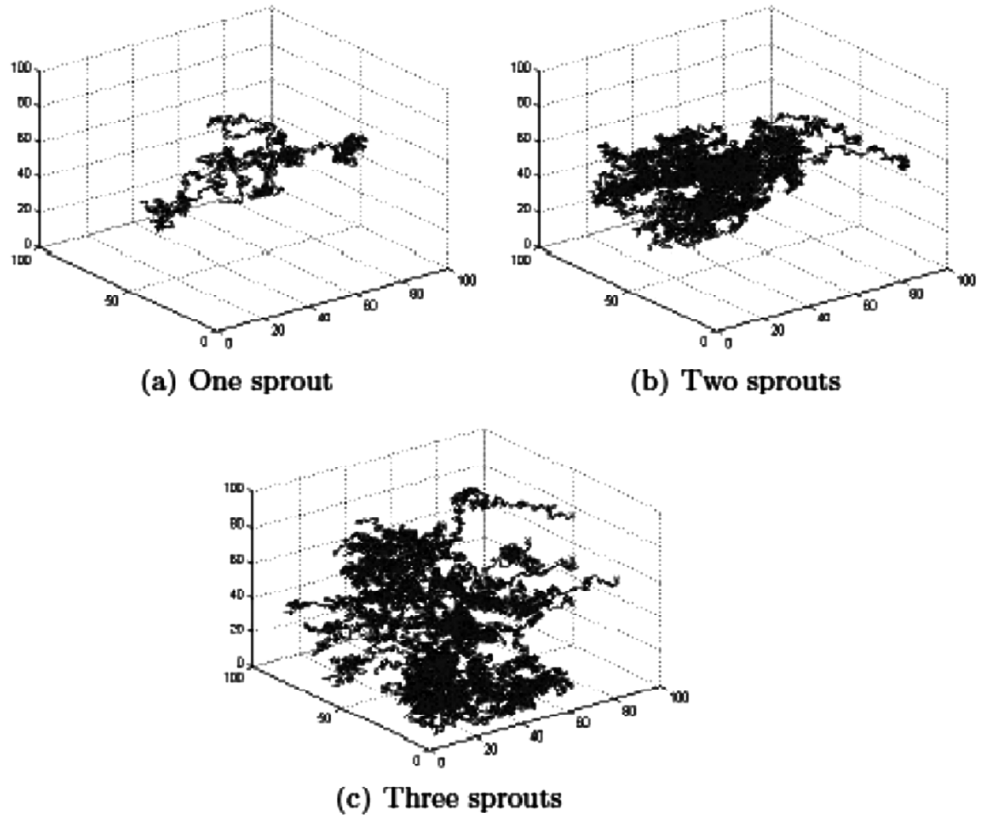

Figure 8: Three-Dimensional Random Walk Images for Different Number of Sprouts

In three dimensions, in Fig. 8 we observe the random walks with one, two and three sprouts, where again the brush border effect as well as the tip proliferation and the attraction towards the tumor become visible.

4. Comparison to Real Data

4.1 Two-Dimensional Scans

Angiography allows to visualize the lumen of blood vessels and organs of the body by injecting a radioopaque contrast agent into the blood vessel and producing images using X-ray based techniques. The most widely used method for assessing tumor angiogenesis is quantification of the micro vessel density with microscopy of a biopsy specimen, however, several imaging methods (e.g., magnetic resonance imaging, computed tomography and spectroscopy) may be used to evaluate the degree of angiogenesis indirectly by measuring a parameter or a combination of parameters such as vascular density, blood flow, blood volume, and/or vascular permeability.

In this work we have experimental evidence available of angiogenesis in a variety of cancers; in the pictures of Figs. 9 and 10, a contrast dye has been injected in the feeder arteries in order to make the entire tumor vascularization visible. The Figures have been produced at the Eberhard-Karls-University Tübingen (Germany), at the Department of Radiology.

Figure 10 shows further angiographic scans, in which a liver carcinoma with its feeder vessels (formed by angiogenesis) is displayed. Note how the newly formed vessels are branching as they are nearing the tumor mass. These images have been taken after successful angiogenesis; they show some relevant characteristics of tumor vessels, which we expect to see also in our model. Note that the more enhanced a vessel, the more it is perfused.

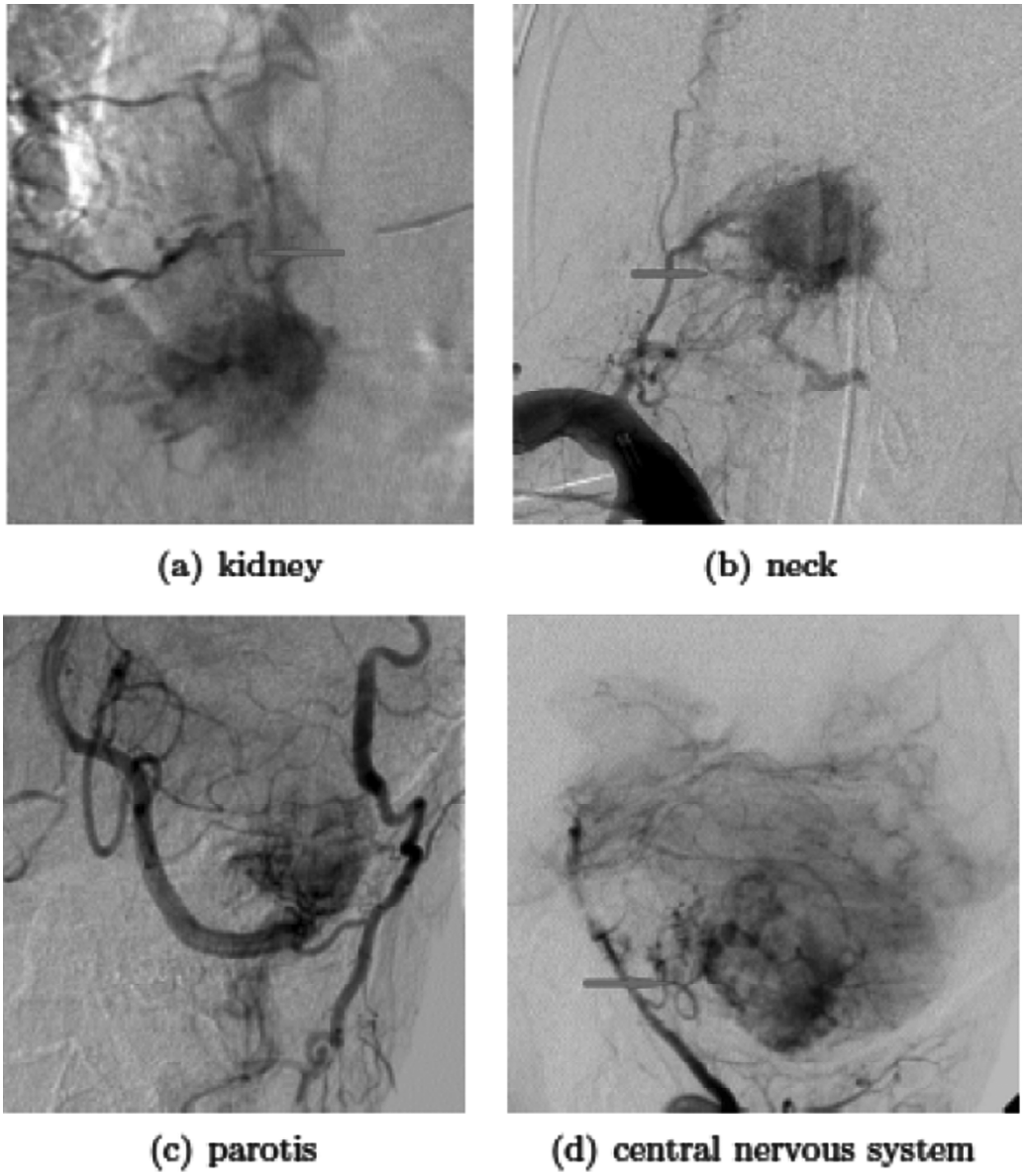

Figure 9: Contrast-Enhanced Angiographic Scans as Angiogenesis Develops in Several Types of Tumor

In order to help understand how angiogenesis functions, one could interpret the spread of contrast dye as angiogenesis. In Fig. 10(a) we can see the vessel from which later the sprouts will direct towards the tumor. In the next subfigures, one can see the tumor with its vessels that have been formed by angiogenesis and are now invading this mass. Throughout the image series, more and more smaller vessels that have originated from the larger vessels, can now be seen. They all are directing towards the main tumor mass. This behavior is displayed in the model's simulation by branching, see Figs. 7 and 8. In addition, it should be noted that the vessels directing towards the tumor become more and more straight as they approach the tumor.

Another particular behavior to observe is the so-called brush border effect reproduced first by Muthukkarpuppan *et al*. [40]. This can also be seen in the model's simulations. Characteristics of the brush border effect are on the one hand, the maximal tip density must lay behind the leading tip front and this magnitude must increase with the proximity to the tumor. On the other hand, the maximal tip density must lie in front of the maximal vessel density. We have reproduced and shown all of these important effects in our model, which may be seen in the section on numerical results.

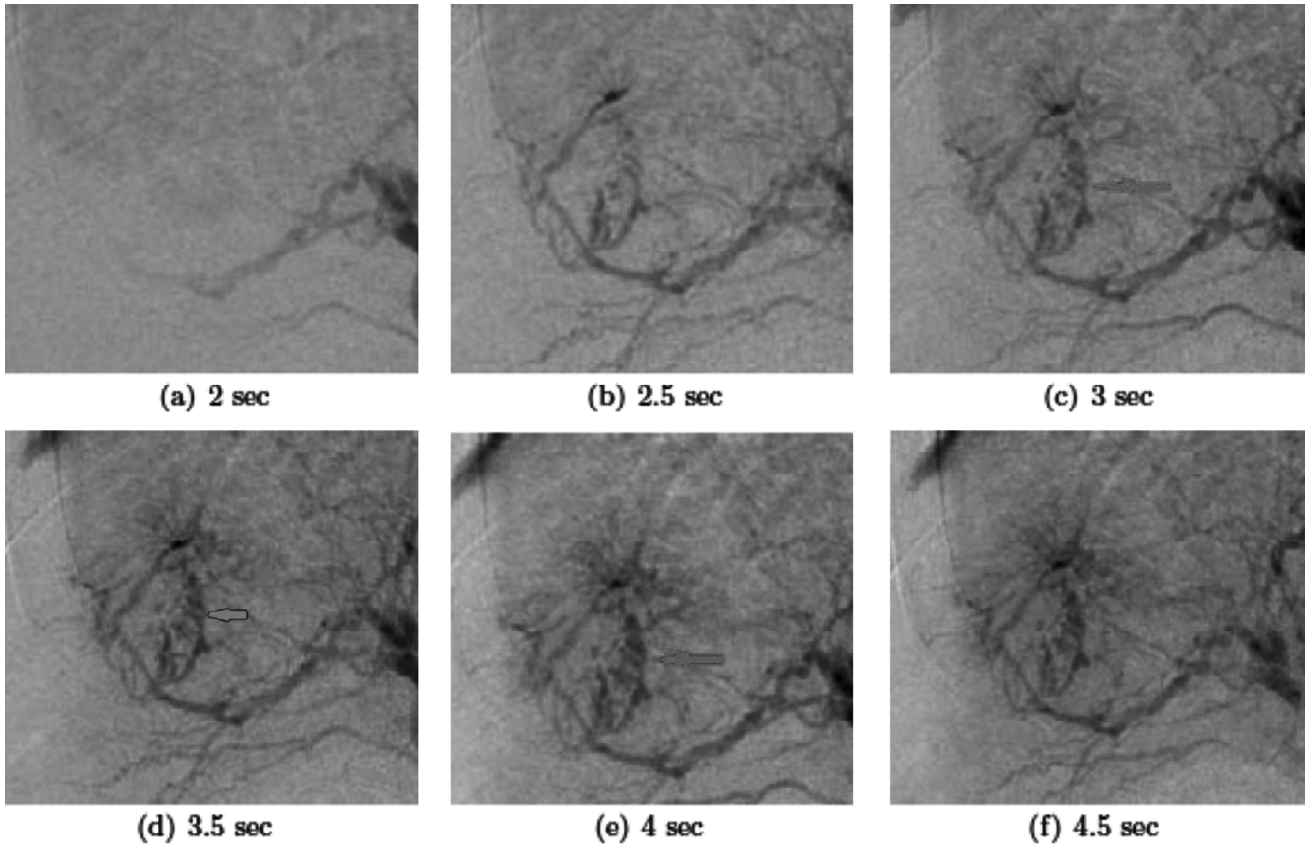

Figure 10: Contrast-Cnhanced Angiographic Scans as Angiogenesis Develops in Liver Carcinoma

Further we can observe that, depending on the consistency of the tissue, there is more or less collateral movement, e.g. in a “hard” tissue like the neck one can see a lot of side movement unlike in a “soft” tissue like the kidney, where there are more straight lines towards the tumor, compare the red arrows in Fig. 9.

5. Conclusions

A main component in tumor development is the process of angiogenesis, in which from already existing vessels, new vessels are being formed. Angiogenesis begins with chemotactic factors that are secreted by the tumor. In response to this, vessel arousal and growth begin. In this paper, we have developed a consistent model for the process of angiogenesis in up to three dimensions. In order to do so, we first developed a continuous mathematical model consisting of partial differential equations, describing the evolution of the concentration of the endothelial cells as well as the concentrations of the tumor angiogenesis factors (TAF), the fibronectin and the matrix degenerating enzyme (MDE). A special feature of our model is the use of porous medium diffusion as well as Monod growth terms, which proved to be useful as it enabled us to observe the brush border effect and the tip proliferation without using Heaviside functions as a natural result of the system of partial differential equations. Furthermore, the strong attraction of the sprouts by the tumor becomes visible. From our numerical results, one could hypothesize that not only the tip proliferation is a reason for the brush border effect and the sudden increase of the EC density at certain concentration values but also the density of the tissue, which is modeled by the inclusion of porous medium diffusion.

In a second step, we developed a discrete mathematical random walk model based on the evolution of the substances and EC from the continous mathematical model. In this part, the exact movement of the tips towards the tumor is modeled by a random walk. We described the movement of the EC dependent on the transition probabilities we calculated. This modeling approach allows to describe angiogenesis with the help of a certain selection of transition probabilities, which enables description of microscopic processes.

Despite so many simplifications, our numerical simulations can show realistic networks generated by angiogenesis and their development during different time steps. Connections between vessels and new branching, out of existing sprouts, can be displayed. Furthermore, we compared simulation results obtained when using porous medium diffusion with simulation results obtained with Fickian diffusion. In these results, the effects of the use of porous medium diffusion became obvious. Further, we observed that there is more collateral movement if the 6 is higher, i.e., if the tissue is “harder”, compare Fig. 7.

In the last part we compared our results to real data and found that our model is able to generate networks that ressemble those generated by angiogenesis *in vivo*. Thus we can conclude that our model includes the most important factors that influence angiogenesis.

The inclusion of more factors that might influence angiogenesis would not change the qualitative behaviour of the system.

Nevertheless our model might be improved further by performing a complete parameter estimation based on real data in order to estimate the parameters in such a way that we can predict the quantitative behaviour of the system.

APPENDIX

Table of Parameters

Table of Parameters

Parameter	*Description*	*Value*
D_n	Diffusion rate of EC	0.1
n_0	Initial value	1
σ	Exponent of porous medium diffusion of EC	4
χ_0	Chemotaxis coefficient	1
φ	Haptotaxis coefficient	0.004
κ	Death rate of EC	5
μ_2	Growth rate of EC	20
γ_2	Monod growth substrate concentration	0.7
D_c	Diffusion rate of TAF	1
δ	Death rate of TAF	1
α_1	Growth rate of TAF-consumption	10
γ_1	Monod growth substrate concentration	1
β	Production rate of fibronectin	5
μ	Degradation rate of fibronectin	0.1
η	Degradation rate of fibronectin	1
α	Production coefficient of MDE	1
τ	Diffusion coefficient of MDE	1
ν	Decay rate of MDE	1
f_0	Initial value	1

AUTHOR’S CONTRIBUTIONS

Thomas Horger, Aenne Oelker, Christina Kuttler and Judith Pérez-Velázquez designed the mathematical part, ran the simulations and wrote the manuscript.

ACKNOWLEDGEMENTS

We would like to thank Prof. Dr. med. Marius Horger, Department of Radiology, Eberhard-Karls-University Tübingen (Germany) for providing the experimental data.

References

[1] Davis B., Reinforced Eandom Walk, *Probability Theory and Related Fields*, (1990), **84**, 203-229.

[2] Sleeman B., and Wallis I. P., (2002), Tumour Induced Angiogenesis as a Reinforced Random Walk: Modelling Capillary Network Formation Without Endothelial Cell Proliferation, *Mathematical and Computer Modelling*, **36**(3), 339-358.

[3] Kerbel R. S., (2002), Tumor Angiogenesis: Past, Present and the Near Future, *Carcinogenesis*, **21**(3), 505-515.

[4] Folkman J., (1971), Tumor Angiogenesis: Therapeutic Implications, *New England Journal of Medicine*, **285**(21), 1182-1186.

[5] Ausprunk D. H., and Folkman J., (1977), Migration and Proliferation of Endothelial Cells in Preformed and Newly Formed Blood Vessels During Tumor Angiogenesis, *Microvascular Research*, **14**(1), 53-65.

[6] Muthukkaruppan V., and Auerbach R., (1979), Angiogenesis in the Mouse Cornea, *Science*, **205**(4413), 1416-1418.

[7] Carmeliet P., (2005), Angiogenesis in Life, Disease and Medicine, *Nature*, **438**, 932-936.

[8] Levine H., and Sleeman B. D., (2003), Modelling Tumour-Induced Angiogenesis, *Cancer Modelling and Simulation*.

[9] Levine H., Sleeman B. D., and Nilsen-Hamilton M., (2001), Mathematical Modeling of the Onset of Capillary Formation Initiating Angiogenesis, *Journal of Mathematical Biology*, **42**, 195-238.

[10] Levine H. A., Pamuk S., Sleeman B. D., and Nilsen-Hamilton M., (2001), Mathematical Modeling of Capillary Formation and Development in Tumor Angiogenesis: Penetration into the Stroma, *Bulletin of Mathematical Biology*, **63**(5), 801-863.

[11] Levine H. A., Sleeman B. D., and Nilsen-Hamilton M., (2000), A Mathematical Model for the Roles of Pericytes and Macrophages in the Initiation of Angiogenesis. i. The Role of Protease Inhibitors in Preventing Angiogenesis, *Mathematical Biosciences*, **168**(1), 77-115.

[12] Plank M., and Sleeman B., (2004), Lattice and Non-Lattice Models of Tumour Angiogenesis, *Bulletin of Mathematical Biology*, **66**, 1785-1819.

[13] Plank M. J., and Sleeman B. D., (2003), A Reinforced Random Walk Model of Tumour Angiogenesis and Anti-Angiogenic Strategies, *Mathematical Medicine and Biology*, **20**(2), 135-181.

[14] Plank M. J., Sleeman B. D., and Jones P. F., (2002), A Mathematical Model of an in Vitro Experiment to Investigate Endothelial Cell Migration, *Journal of Theoretical Medicine*, **4**(4), 251-270.

[15] Plank M. J., Sleeman B. D., and Jones P. F., (2004), A Mathematical Model of Tumour Angiogenesis, Regulated by Vascular Endothelial Growth Factor and the Angiopoietins, *Journal of Theoretical Biology*, **229**(4), 435-454.

[16] Plank M. J., Sleeman B. D., and Jones P. F., (2004), The Role of the Angiopoietins in Tumour Angiogenesis, *Growth Factors*, **22**(1), 1-11.

[17] Othmer H. G., and Stevens A., (1997), Aggregation, Blowup, and Collapse: The abc's of Taxis in Reinforced Random Walks, *SIAM Journal on Applied Mathematics*, **57**, 1044-1081

[18] Mantzaris N. V., Webb S., and Othmer H. G., (2004), Mathematical Modeling of Tumor-Induced Angiogenesis, *Journal of Mathematical Biology*, **49**, 111-187.

[19] McDougall S. R., Anderson A. R. A., and Chaplain M. A. J., (2006), Mathematical Modelling of Dynamic Adaptive Tumor-Induced Angiogenesis: Clinical Implications and Therapeutic Targeting Strategies, *Journal of Theoretical Biology*, **241**, 564-589.

[20] Chaplain M. A. J., (2000), Mathematical Modelling of Angiogenesis, *Journal of Neuro-Oncology*, **50**, 37-51.

[21] Anderson A. R. A., Chaplain M. A. J., García-Reimbert C., and Vargas C. A., (2000), A Gradient-Driven Mathematical Model of Antiangiogenesis, *Mathematical and Computer Modelling*, **32**, 1141-1152.

[22] Balding D., and McElwain D. L. S., (1985), A Mathematical Model of Tumour-Induced Capillary Growth, *Journal of Theoretical Biology*, **114**(1), 53-73.

[23] Byrne H. M., and Chaplain M. A. J., (1995), Mathematical Models for Tumour Angiogenesis: Numerical Simulations and Nonlinear Wave Solutions, *Bulletin of Mathematical Biology*, **57**, 461-486.

[24] Chaplain M. A. J., (1996), Avascular Growth, Angiogenesis and Vascular Growth in Solid Tumours: The Mathematical Modelling of the Stages of Tumour Development, *Mathematical and Computer Modelling*, **23**(6), 47-87.

[25] Valenciano J., and Chaplain M., (2003), Computing Highly Accurate Solutions of a Tumour Angiogenesis Model, *Mathematical Models and Methods in Applied Sciences*, **13**, 747-766.

[26] Orme M. E., and Chaplain M. A. J., (1996), A Mathematical Model of the First Steps of Tumour-Related Angiogenesis: Capillary Sprout Formation and Secondary Branching, *Mathematical Medicine and Biology*, **13**(2), 73-98.

[27] Stéphanou A., McDougall S. R., Anderson A. R. A., and Chaplain M. A. J., (2005), Mathematical Modelling of Flow in 2d and 3d Vascular Networks: Applications to Anti-Angiogenic and Chemotherapeutic Drug Strategies, *Mathematical and Computer Modelling*, **41**(10), 1137-1156.

[28] Anderson A. R. A., and Chaplain M. A. J., (1998), Continuous and Discrete Mathematical Models of Tumor-Induced Angiogenesis, *Bulletin of Mathematical Biology*, **60**, 857-899.

[29] Travasso R. D. M., Corvera Poira E., Castro M., Rodriguez-Manzaneque J. C., and Hernández-Machado A., (2011), Tumor Angiogenesis and Vascular Patterning: A Mathematical Model. PLoS ONE 2011, 6(5).

[30] Schoeld J. W., Ganey E. A., Gatenby R. A., and Maini P. K., (2011), Tumour Angiogenesis: The Gap Between Theory and Experiments, *Journal of Theoretical Biology*, **274**(1), 97-102.

[31] Peirce S. M., (2008), Computational and Mathematical Modeling of Angiogenesis, *Microcirculation*, **15**(8), 739-751.

[32] Alarcon T., (2009), Modelling Tumour-Induced Angiogenesis: A Review of Individual-Based Models and Multi-Scale Approaches, In Mathematics, Developmental Biology and Tumour Growth: UIMP-RSME Luis A. Santaló Summer School, September 11-15, 2006, Universidad Internacional Menéndez Pelayo, Santander, Spain. Edited by Giráldez F, Herrero M, Pelayo UIM, American Mathematical Society, (2009).

[33] McDougall S. R., and Sorbie K., (1997), The Application of Network Modelling Techniques to Multiphase Flow in Porous Media, *Petroleum Geoscience*, **3**, 161-169.

[34] Levine H. A., Pamuk S., Sleeman B. D., and Nilsen-Hamilton M., (2002), Mathematical Modelling of Tumour Angiogenesis and the Action of Angiostatin as a Protease Inhibitor, *Journal of Theoretical Medicine*, **4**, 133-145.

[35] Zheng X., Wise S., and Cristini V., (2005), Nonlinear Simulation of Tumor Necrosis, Neo-Vascularization and Tissue Invasion via an Adaptive Finite-Element/Level-Set Method, *Bulletin of Mathematical Biology*, **67**, 211-259.

[36] Sleeman B. D., and Levine H. A., (2001), Partial Differential Equations of Chemotaxis and Angiogenesis, *Mathematical Methods in the Applied Sciences*, **24**, 405-426.

[37] Ambrosi D., and Preziosi L., (2002), On the Closure of Mass Balance Models for Tumor Growth, *Mathematical Models and Methods in Applied Sciences*, **12**, 737-754.

[38] Byrne H. M., and Preziosi L., (2003), Modelling Solid Tumour Growth Using the Theory of Mixtures, *Mathematical Medicine and Biology*, **20**, 341-366.

[39] Habbal A., (2004), A Nash Topology Game for Tumoral Anti-Angiogenesis, *Tech. Rep.*, RR-5252, INRIA.

[40] Muthukkaruppan V. R., Kubai L., and Auerbach R., (1982), Tumor-Induced Neovascularization in the Mouse Eye, *Journal of the National Cancer Institute*, **69**(3), 699-708.